Numerical study of the effect of dynamic capillary pressure in porous medium

Fučík, Radek
Department of Mathematics, Faculty of Nuclear Sciences and Physical Engineering, Czech Technical University

Mikyška, Jiří
Department of Mathematics, Faculty of Nuclear Sciences and Physical Engineering, Czech Technical University

Sakaki, Toshihiro
Department of Environmental Science and Engineering, Colorado School of Mines

Illangasekare, Tissa H.
Department of Mathematics, Faculty of Nuclear Sciences and Physical Engineering, Czech Technical University

出版情報：COE Lecture Note. 14, pp.14-30, 2009-02-12. Faculty of Mathematics, Kyushu University
バージョン：
権利関係：

Proceedings of the Czech-Japanese Seminar in Applied Mathematics 2008
Takachiho / University of Miyazaki, Miyazaki, Japan, September 1-7, 2008
pp. 14-30

NUMERICAL STUDY OF THE EFFECT OF DYNAMIC CAPILLARY PRESSURE IN POROUS MEDIUM

RADEK FUČÍK[1], JIŘí MIKYŠKA[1], TOSHIHIRO SAKAKI[2], TISSA H. ILLANGASEKARE[2]

Abstract. In order to investigate effects of the dynamic capillary pressure-saturation relationship used in the modelling of flow in porous medium, a one-dimensional fully implicit numerical scheme is proposed and its validity is discussed by means of semi-analytical solutions developed by McWhorter and Sunada and by the authors. The numerical scheme is used to simulate experimental procedure using the measured dataset for the sand and fluid properties. Results of the simulation using different models for dynamic effect term in capillary pressure - saturation relationship are presented and discussed.

1. Introduction. In the understanding and prediction of the flow of immiscible and incompressible fluids in porous medium, a reliable model of capillary forces acting on the fluids is crucial. In past decades, various capillary pressure - saturation models were correlated from laboratory experiments in equilibrium conditions. These static capillary pressure - saturation relationships such as [4] or [28] has been used in almost all mathematical studies on modelling of multiphase flow in porous medium. However, soil physicists found that the laboratory measured capillary pressure does not correspond to capillary pressure in case of large velocities. Recently, as a result of the empirical approach in [26], theoretical studies [13], [14], [16], [15], [7], or [3] have produced new aspects in the two-phase flow theories. The most important result is that the classical capillary pressure - saturation relationship holds only in the state of thermodynamic equilibrium. Therefore, it is believed that the classical approach cannot be used in the modelling of capillarity when the fluid content is in motion and a new model of the capillary pressure - saturation relationship is proposed, i.e., the dynamic capillary pressure,[13], [14], [16], [15].

This manuscript focuses on the implications of the dynamic capillary pressure - saturation relationship. The fully implicit numerical scheme is proposed and validated using the (semi-)analytical solutions for the static capillary pressure [22], [10], and [11]. By estimating the experimental order of convergence, it is shown that the numerical scheme is convergent and can be used for simulating flow in both homogeneous and heterogeneous porous medium. Consequently, the inclusion of various models of dynamic capillary pressure coefficient are investigated and compared to the static model of capillary pressure.

The two phase flow system can be simplified to the Richards problem, where the pressure of the non-wetting phase (air or oil) is assumed to be constant. This is the case in [18], where the dynamic effects is found not to be relevant for the given structure of heterogeneous porous medium. Other numerical approaches using the dynamic capillary pressure have been already studied for instance in [21], [20], or [24]. However, the relevance of using the dynamic capillary pressure in the full two-phase flow system of equations has not been answered yet. The presented fully implicit

[1]Department of Mathematics, Faculty of Nuclear Sciences and Physical Engineering, Czech Technical University, Prague.
[2]Department of Environmental Science and Engineering, Colorado School of Mines, Golden, Colorado.

numerical scheme can be used for such a detailed investigation of the saturation and capillary pressure behaviour when dynamic capillary pressure is used instead of the static capillary pressure in the full two-phase flow system. Moreover, different models for the dynamic capillary pressure - saturation relationship are employed and their respective impacts are discussed.

In this section, the constitutive quantities are introduced and the capillary pressure is defined. Thorough definitions, descriptions, and examples can be found in [8], [20], [1], [17], or [2]. Then, the mathematical model and the numerical scheme is presented in Section 2. In the last section, the numerical scheme is validated using analytical and semi-analytical solutions and the numerical experiments with dynamic capillary pressure model are discussed.

1.1. Saturation. The fluid distribution in immiscible multiphase flow in porous media is described by the saturation S_α $[-]$[1] which indicates the volumetric portion of the void space within the pores occupied by the fluid phase α. Hence, S_α is always between 0 and 1. The sum of saturations S_α of all fluids present in the porous media is 1, i.e., $\sum_\alpha S_\alpha = 1$.

Since not all volume of the fluid phase can be displaced in the multiphase flow from the porous medium, the α-phase residual saturation quantity $S_{r\alpha}$ $[-]$ is introduced. It expresses the minimal saturation of the phase α that will retain in porous medium due to adhesion effects with respect to the solid matrix. Consequently, the effective saturation S_α^e $[-]$ that describes only volumetric portions of displaceable fluid phases is introduced as

$$S_\alpha^e = \frac{S_\alpha - S_{r\alpha}}{1 - \sum_\beta S_{r\beta}}. \tag{1.1}$$

1.2. Capillary pressure. Following the standard definitions in literature, the capillary pressure p_c $[ML^{-1}]$ on the pore scale is defined as the difference between the non-wetting phase pressure p_n $[ML^{-1}]$ and the wetting phase pressure p_w $[ML^{-1}]$, i.e.,

$$p_c = p_n - p_w. \tag{1.2}$$

On the macroscale, the capillary pressure has been commonly considered as a function of wetting phase saturation only and it has been widely used in model equations in literature [17], [2], [23], [12], [9], or [10]. The following Brooks and Corey [4] capillary pressure - effective wetting phase saturation parameterization is used in the presented two-phase flow model [2]

$$p_c^{eq} = p_d (S_w^e)^{-\frac{1}{\lambda}}, \tag{1.3}$$

where p_d $[ML^{-1}]$ is the entry pressure and λ $[-]$ describes the pore distribution of the grains in porous material. The Brooks and Corey relationship (1.3) is suitable for modelling of flow in heterogeneous porous media because the difference in the entry pressure coefficients p_d in different porous materials captures the barrier effect that has been observed in experiments [23], [17], [1], [8]. As the main objective of

[1] [ ] indicates the unit of a symbol.

[2] A superscript ^{eq} is used in the definition (1.3) with respect to the latter and it indicates the capillary pressure - saturation relationship model in thermodynamic equilibrium.

the ongoing research is to study the capillarity in heterogeneous porous media, other capillary pressure - saturation models (like that by van Genuchten [28] which does not include the barrier effect) will not be considered in this manuscript.

The dynamic capillary pressure - saturation relationship is proposed in the following form [14]:

$$p_c := p_n - p_w = p_c^{eq} - \tau \frac{\partial S_w}{\partial t}, \tag{1.4}$$

where p_c^{eq} is the capillary pressure - saturation relationship in the thermodynamic equilibrium of the system (referred to as the static capillary pressure) and τ $[ML^{-1}T^{-1}]$, the dynamic effect coefficient, is a material property of the system.

Early in 1978, before the thermodynamic definition of (1.4) in [14], Stauffer [26] observed the dynamic effect in laboratory experiments and proposed a linear dependence in (1.4) with the following definition of τ

$$\tau_S = \frac{\alpha_S \mu_w \Phi}{K\lambda} \left(\frac{p_d}{\rho_w g} \right)^2, \tag{1.5}$$

where $\alpha_S = 0.1$ denotes a scaling parameter. Both λ and p_d are the Brooks and Corey parameters [4] that can be experimentally estimated. Other symbols are described in Table 5.1.

The Stauffer model for the dynamic effect coefficient τ_S was obtained by correlating experimental data. The values of τ_S vary between $\tau_S = 2.7 \cdot 10^4$ $Pa\,s$ and $\tau_S = 7.7 \cdot 10^4$ $Pa\,s$, see [20, page 27]. However, other researchers suggest that the magnitude of τ should be in the order of $10^2 - 10^3$ $Pa\,s$, [6], or, on the other hand, it should be also in the order of $10^4 - 10^8$ $Pa\,s$ as estimated in [15].

Recently, a more general nonlinear dependence $\tau = \tau(S_w)$ is assumed to be more relevant in the modelling of realistic two-phase flow displacement [25]. In this manuscript, constant, linear, and loglinear model will be used in numerical simulations in order to investigate their influence on the two-phase flow.

1.3. Interface of porous media. At the interface of two different porous media, the normal components of fluxes of both fluids present in the system are continuous due to conservation of mass [17]. If the fluid phase is present at the interface, its pressure is also continuous. Consequently, following the definition (1.2), the capillary pressure is continuous across the interface. In the case of the dynamic capillary pressure (1.4), this condition yields

$$p_c^{eq,I} - \tau^I \frac{\partial S_w^I}{\partial t} = p_c^{eq,II} - \tau^{II} \frac{\partial S_w^{II}}{\partial t}, \tag{1.6}$$

where the superscripts I and II enumerate the two different porous media, respectively. As a consequence of the continuity of capillary pressure (both static and dynamic), saturation S_α can be discontinuous across the interface, see [17] or [1].

2. Mathematical model. The mathematical model describing the two-phase flow in a one-dimensional domain is presented in this section. The aim is to investigate how the inclusion of the dynamic capillary pressure (1.4) instead of the static relationship (1.3) influences the numerical solution of the resulting system of equations.

2.1. Governing equations. The governing two-phase flow equations in one-dimensional domain $[0, L]$ are given by the $p_w - S_n$ formulation [1]:

$$\Phi \frac{\partial S_\alpha}{\partial t} = \frac{\partial}{\partial x}\left[\frac{K}{\mu_\alpha} k_{r\alpha}\left(\frac{\partial}{\partial x}(p_w + \delta_{\alpha n} p_c) - \rho_\alpha\, g\right)\right], \tag{2.1}$$

where $S_w + S_n = 1$, $\delta_{\alpha n}$ is the Kronecker symbol, and $\alpha \in \{w, n\}$. The wetting (water) and non-wetting fluid (air, NAPL[3]) are indexed by w and n, respectively. The initial and boundary conditions for (2.1) are given for each experimental problem, separately.

2.2. Discrete problem. A standard finite volume discretization technique is used in order to determine approximate discrete solution $S^k_{n,i}$, $p^k_{w,i}$ of the problem (2.1), generally defined as $f^k_i = f(k\Delta t, i\Delta x)$, where $i = 0, 1, \ldots, m$, $m\Delta x = L$, and $k = 0, 1, \ldots, n$, $n\Delta t = T$. L $[L]$ is the length of the domain and T $[T]$ is the final time of the simulation.

Since the nonlinear problem (2.1) involves the dynamic capillary pressure function defined in (1.4) that includes time derivative of S_n, an implicit numerical scheme is proposed in the following form:

$$\Phi \frac{S^{k+1}_{\alpha,i} - S^k_{\alpha,i}}{\Delta t} = -\frac{u^{k+1}_{\alpha,i+1/2} - u^{k+1}_{\alpha,i-1/2}}{\Delta x}, \tag{2.2}$$

where $\alpha \in \{w, n\}$ and the discrete Darcy velocities u_α are given as follows

$$u^{k+1}_{\alpha,i+1/2} = -\frac{K}{\mu_\alpha} k_{r\alpha}(S^{k+1}_{\alpha,upw})\Big(\underbrace{\frac{p^{k+1}_{w,i+1} - p^{k+1}_{w,i}}{\Delta x} + \delta_{\alpha n}\frac{p^{k+1}_{c,i+1} - p^{k+1}_{c,i}}{\Delta x} - \rho_\alpha\, g}_{\frac{\partial}{\partial x}\Phi_\alpha}\Big), \tag{2.3}$$

$$p^{k+1}_{c,i} = p_c\left(1 - S^{k+1}_{n,i}, -\frac{S^{k+1}_{n,i} - S^k_{n,i}}{\Delta t}\right).$$

$S^{k+1}_{\alpha,upw}$ is the saturation taken in the upstream direction with respect to the gradient of the phase potential Φ_α, i.e.

$$S^{k+1}_{\alpha,upw} = \begin{cases} S^{k+1}_{\alpha,i+1} & \text{if } \frac{\partial}{\partial x}\Phi_\alpha \geq 0. \\ \\ S^{k+1}_{\alpha,i} & \text{if } \frac{\partial}{\partial x}\Phi_\alpha < 0. \end{cases}$$

At the material interface, the continuity of capillary pressure (1.6) requires that there is a jump in saturation. Such discontinuous saturation $S_{n,i}$ is represented by $S^I_{n,i}$ and $S^{II}_{n,i}$ as it is shown in Figure 2.1, where i is the index of the node located at the material interface. Therefore, the equation (1.6) is approximated by

$$\begin{aligned} p_c^{eq,I}(1 - S^{k+1,I}_{n,i}) + \tau^I(1 - S^{k+1,I}_{n,i})\frac{S^{k+1,I}_{n,i} - S^{k,I}_{n,i}}{\Delta t} = \\ p_c^{eq,II}(1 - S^{k+1,II}_{n,i}) + \tau^{II}(1 - S^{k+1,II}_{n,i})\frac{S^{k+1,II}_{n,i} - S^{k,II}_{n,i}}{\Delta t}. \end{aligned} \tag{2.4}$$

If $\tau = 0$, the interfacial saturations $S^I_{n,i}$ and $S^{II}_{n,i}$ can be computed analytically by inverting the static capillary pressure function p_c^{eq} defined in (1.3). Therefore, it

[3]Non-Aqueous Phase Liquid

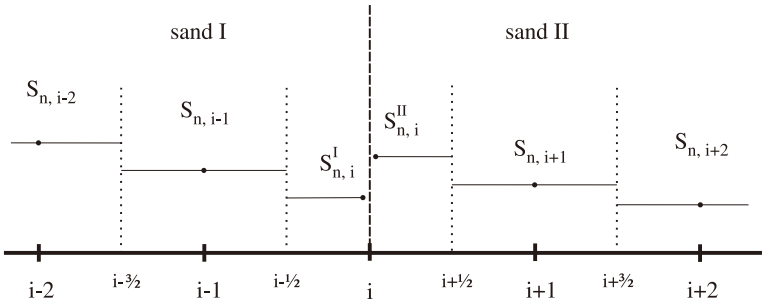

FIG. 2.1. *Discretization of the saturation jump at material discontinuity.*

is sufficient to store only the interfacial saturation that corresponds to the medium with a lower entry pressure p_d because the other one can be easily computed when needed, for details see [17].

However, if $\tau \neq 0$, equation (2.4) is a nonlinear equation that couples $S^I_{n,i}$ and $S^{II}_{n,i}$ and, moreover, the interfacial saturations from the previous time step are also required in (2.4). Consequently, using only one interfacial saturation to represent the numerical solution is insufficient. Hence, $S^I_{n,i}$ and $S^{II}_{n,i}$ are added into the set of unknowns instead of $S_{n,i}$. At the interfacial node i, $S^I_{n,i}$ is used in (2.3) when computing the velocity $u^{k+1}_{\alpha,i-1/2}$, while $S^{II}_{n,i}$ is used in $u^{k+1}_{\alpha,i+1/2}$. Such an increase of unknowns is compensated by the inclusion of (2.4) in the system of equations (2.2) such that the number of unknowns equals to the number of equations.

If the capillary pressure function $p^{eq}_c(S_w)$ is strictly decreasing as in the case of the Brooks and Corey model (1.3), the function evaluated at both sides of (2.4)

$$f(\xi) = p^{eq}_c(1-\xi) + \tau(1-\xi)\frac{\xi - S^{k,I}_{n,i}}{\Delta t} \tag{2.5}$$

is strictly increasing if $\tau(\xi)$ is a non-decreasing function of ξ. Thus, the existence of the inverse function f^{-1} is guaranteed and the equation (2.4) does not alter the convergence of the numerical scheme.

The numerical scheme is solved using the Newton-Raphson iteration method, where the Jacobi matrix is block tridiagonal. In each iteration, the upstream saturation in (2.3) is recomputed using the current iteration of the solution and the interfacial capillary pressure condition (2.4) is solved numerically together with (2.2) and (2.3).

3. Numerical experiments. The numerical scheme (2.2) is validated using analytical and semi-analytical solutions that are available only for the static capillary pressure model and no gravity, i.e. $\tau = 0$ and $g = 0$. The reliability of the numerical solution is determined for three different situations where the advective, diffusive, and both advective and diffusive part of the two-phase flow equations are benchmarked, respectively (Sections 3.1, 3.2, and 3.3). The experimental orders of convergence eoc_k are computed using the L_k norm of the difference between the numerical and the (semi-)analytical solution at the final time of the simulation, where $k = 1, 2$.

In the case of a porous medium with a single discontinuity, the implementation of the interfacial condition (2.4) is verified using the semi-analytical solution developed by the authors [11]. Details are shown in Sections 3.4 and 3.5.

The Ohji sand was used as a porous medium in the following numerical simulations with water and air as a wetting and non-wetting fluid, respectively. Physical properties of the sand shown in Table 3.1 were measured during the laboratory experiments held in the Center for Experimental Study of Subsurface Environmental Processes, Colorado School of Mines. The details of the fluid properties are shown in Table 3.3.

Except for the pure advection problem, the numerical solution is computed also for the models of the dynamic capillary pressure (1.4). The value of the dynamic effect coefficient $\tau = \tau(S_w)$ was estimated as a result of the laboratory experiment, where capillary pressure and time evolution of the water saturation were measured. Three functional models of the dynamic effect coefficient $\tau = \tau(S_w)$ were correlated, see Table 3.2. Additionally, the Stauffer model (1.5) gives $\tau_S = 3.3 \cdot 10^5$ for the Ohji sand. In the following subsections, the numerical solutions using these dynamic capillary pressure models are compared to the referential numerical solution computed with the static capillary pressure model $p_c \equiv p_c^{eq}$ (1.3).

Unfortunately, no laboratory data is available for the case of a simple heterogeneous porous medium described in Sections 3.4 and 3.5. In order to investigate solutions for the different models of the dynamic effect coefficient $\tau(S_w)$ in a heterogeneous porous medium, a fictive, coarser sand $\text{Ohji}_{0.9}$ is introduced. Its parameters are the same as for the Ohji sand except for the capillary pressure p_c, the intrinsic permeability K, and τ, which are all multiplied by the factor 0.9 (see Table 3.1).

Parameter			Ohji sand	$\text{Ohji}_{0.9}$ sand
Porosity	Φ	$[-]$	0.448	0.448
Intrinsic permeability	K	$[m^2]$	$1.63{\cdot}10^{-11}$	$1.47{\cdot}10^{-11}$
Residual water saturation	S_{wr}	$[-]$	0.265	0.265
Brooks-Corey entry pressure	p_d	$[Pa]$	3450	3105
Brooks-Corey pore size dist. index	λ	$[-]$	4.66	4.66

TABLE 3.1
Properties of the porous media used in the numerical simulation.

Model of τ $[Pa\ s]$	Ohji sand	$\text{Ohji}_{0.9}$ sand
Constant model	$\tau(S_w) = 1.1 \cdot 10^6$	$\tau(S_w) = 9.9 \cdot 10^5$
Linear model	$\tau(S_w) = 3.2 \cdot 10^6(1 - S_w)$	$\tau(S_w) = 2.88 \cdot 10^6(1 - S_w)$
Loglinear model	$\tau(S_w) = 10^8 \exp(-7.7S_w)$	$\tau(S_w) = 9 \cdot 10^7 \exp(-7.7S_w)$

TABLE 3.2
Experimentally determined models of the dynamic effect coefficient τ for the Ohji sand and fictive values of τ for the $\text{Ohji}_{0.9}$ sand.

Parameter			Water	Air
Density	ρ	$[kg\ m^{-3}]$	997.8	1.205
Dyn. viscosity	μ	$[kg\ m^{-1}s^{-1}]$	$9.77 \cdot 10^{-4}$	$1.82 \cdot 10^{-5}$

TABLE 3.3
Fluid properties used in the simulations.

3.1. Pure advection. Assuming $p_c \equiv 0$, the system of equations (2.1) can be simplified into a single hyperbolic equation with $\partial p_\alpha / \partial x = \text{const}$, see [17], [19]. In [5], Buckley and Leverett derived the analytical solution of such a problem using the modified method of characteristics. The problem description is shown in Table 3.4.

Numerical solutions compared to the Buckley and Leverett analytical solutions are shown in Figure 3.1.

Initial condition :	$S_n(x,0) = 0$	$\forall x \in (0, L)$
Boundary conditions :	$S_n(0,t) = 1 - S_{wr} = 0.735$	$\forall t \in [0, T]$
	$S_n(L,t) = 0$	$\forall t \in [0, T]$
	$u_n(L,t) = 10^{-4}$	$\forall t \in [0, T]$
Problem setup :	$T = 1000\ s$, $L = 15\ cm$, $g = 0$, $p_c \equiv 0$	
Porous medium :	Homogeneous porous medium	
Sand :	Ohji sand, Table 3.1	

TABLE 3.4
Description of the pure advection problem

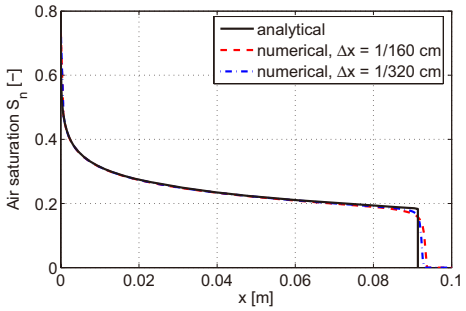

Experimental order of convergence		
$\Delta x\ [cm]$	eoc_1	eoc_2
$1 \rightarrow 1/2$	0.83	0.70
$1/2 \rightarrow 1/4$	0.81	0.71
$1/4 \rightarrow 1/8$	0.80	0.72
$1/8 \rightarrow 1/16$	0.80	0.73
$1/16 \rightarrow 1/32$	0.80	0.72
$1/32 \rightarrow 1/64$	0.80	0.69
$1/64 \rightarrow 1/128$	0.81	0.61

Grid size $\Delta x\ [cm]$	Time step $\Delta t\ [s]$
1	100
$1/2$	$100/2$
$1/4$	$100/4$
$1/8$	$100/8$
$1/16$	$100/16$
$1/32$	$100/32$
$1/64$	$100/64$
$1/128$	$100/128$

FIG. 3.1. *Numerical solutions of the Buckley and Leverett problem (the pure advection case) compared to the analytical solution, $t = 1000\ s$. The experimental order of convergence eoc_1 and eoc_2 are measured in L_1 and L_2 norms, respectively.*

3.2. Pure capillary diffusion in homogeneous medium. If no external forces act on the system, i.e., $g \equiv 0$, the flow in the one-dimensional domain is governed only by capillarity and the system of equations (2.1) can be reformulated to satisfy the McWhorter and Sunada problem formulation for the case of a bi-directional fluid displacement, see [22], [10], [11]. Therefore, the McWhorter and Sunada semi-analytical solution for the pure capillary diffusion problem can be obtained as a benchmark solution for the numerical solution. The problem details are shown in Table 3.5.

As the numerical grid gets finer, the agreement of the numerical solution with respect to the semi-analytical solution is apparent as it is shown in Figure 3.2.

The numerical solutions for the dynamic capillary pressure models are shown in Figure 3.3.

3.3. Advection and capillary diffusion in homogeneous medium. If a flux of air is imposed at the domain boundary, the flow in the domain is governed by both capillarity and advection. Moreover, if the domain is placed horizontally, i.e., $g = 0$, the generalized McWhorter problem formulation can be used in order to

Initial condition :	$S_n(x,0) = 0$	$\forall x \in (0, L)$
Boundary conditions :	$S_n(0,t) = 0.73$	$\forall t \in [0, T]$
	$S_n(L,t) = 0$	$\forall t \in [0, T]$
Problem setup :	$T = 1000\ s$, $L = 1\ m$, $g = 0$	
Capillary pressure :	Classical model (1.3), $p_c \equiv p_c^{eq}$, $\tau \equiv 0$	
Porous medium :	Homogeneous porous medium	
Sand :	Ohji sand, Table 3.1	

TABLE 3.5
Description of the pure capillary diffusion problem in homogeneous porous medium.

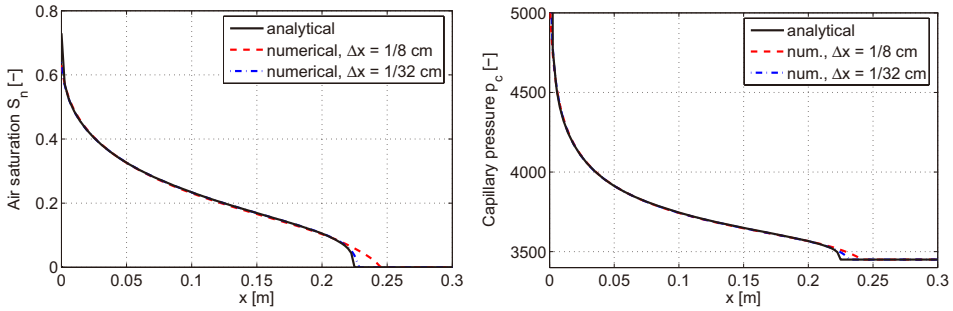

Experimental order of convergence		
Δx $[cm]$	eoc_1	eoc_2
$2 \rightarrow 1$	0.66	0.62
$1 \rightarrow 1/2$	0.73	0.67
$1/2 \rightarrow 1/4$	0.77	0.70
$1/4 \rightarrow 1/8$	0.80	0.72
$1/8 \rightarrow 1/16$	0.82	0.74
$1/16 \rightarrow 1/32$	0.84	0.75

Grid size Δx $[cm]$	Time step Δt $[s]$
2	200
1	50
$1/2$	$50/4$
$1/4$	$50/16$
$1/8$	$50/64$
$1/16$	$50/256$
$1/32$	$50/1024$

FIG. 3.2. *Numerical solutions of the pure capillary diffusion problem compared to the McWhorter and Sunada semi-analytical solution, $t = 1000\ s$. The experimental order of convergence eoc_1 and eoc_2 are measured in L_1 and L_2 norms, respectively.*

obtain semi-analytical solution, which has been discussed by the authors in [10] and [11]. The description of the problem is given in Table 3.6.

The main benefit of such a closed-form solution is a direct comparison of effects of both advection and capillarity on the two-phase flow. The numerical solutions compared to the McWhorter and Sunada semi-analytical solution are shown in Figure 3.4 and, again, the experimental errors of convergence show convergence of the numerical solution towards the exact solution.

The necessity of infinite flux at $t = 0$ requires careful handling of the boundary conditions. Despite singularity at $t = 0$, the entry flux of air, denoted as u_0, is integrable and thus the implementation of such a boundary condition is possible.

The numerical solutions for the dynamic capillary pressure models are shown in Figure 3.5. Compared to the static, linear, or loglinear cases, the inclusion of the constant model of τ in the capillary pressure leads to a non-monotonous profile of $p_c = p_c(x)$.

3.4. Pure capillary diffusion in heterogeneous medium. If the porous medium described in Section 3.2 has a single discontinuity in the material properties,

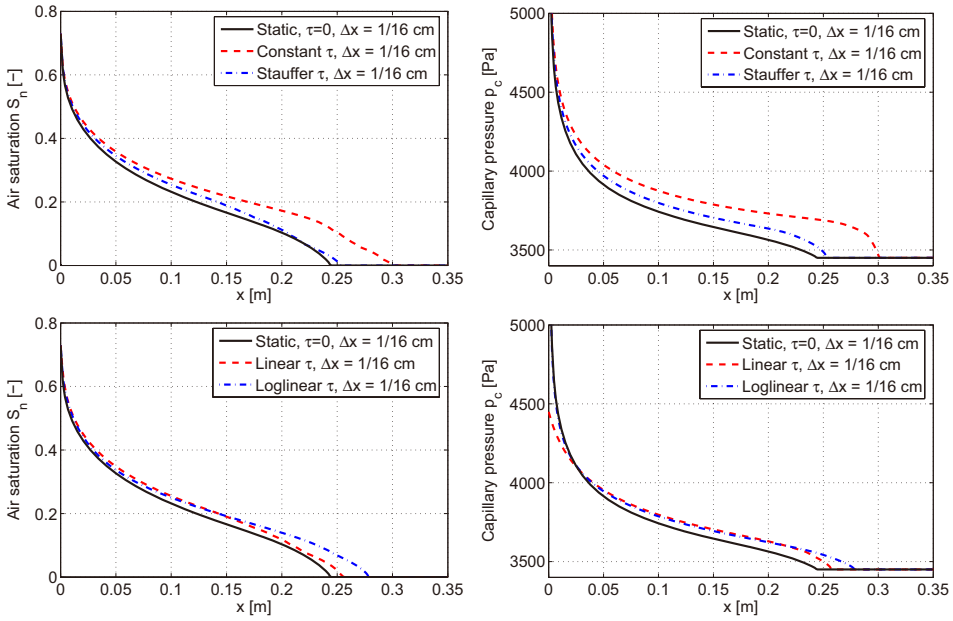

FIG. 3.3. *Numerical solutions of the pure capillary diffusion problem using the constant, linear, and loglinear models for dynamic effect coefficient τ are compared to the numerical solutions obtained for the static capillary pressure $\tau = 0$, $t = 1000$ s.*

Initial condition :	$S_n(x,0) = 0$	$\forall x \in (0, L)$
Boundary conditions :	$S_n(0,t) = 0.73$	$\forall t \in [0, T]$
	$S_n(L,t) = 0$	$\forall t \in [0, T]$
	$u_n(0,t) = u_0(t) = 1.63 \cdot 10^{-3} t^{-1/2}$	$\forall t \in [0, T]$
	$u_w(L,t) = 0.9 u_0(t)$	$\forall t \in [0, T]$
Problem setup :	$T = 1000$ s, $L = 1$ m, $g = 0$	
Capillary pressure :	Classical model (1.3), $p_c \equiv p_c^{eq}$, $\tau \equiv 0$	
Porous medium :	Homogeneous porous medium	
Sand :	Ohji sand, Table 3.1	

TABLE 3.6
Description of the advection and capillary diffusion problem in homogeneous porous medium

i.e., it consists of two homogeneous porous media, the system of equation (2.1) can be reformulated into the van Duijn and de Neef problem formulation [27]. Again, a semi-analytical solution is available to benchmark the numerical solution and it is a special case of the more general family of semi-analytical solutions developed by the authors in [11]. As described in Table 3.7, the material discontinuity is located in the middle of the domain at $L/2$.

The numerical solutions compared to the semi-analytical solution are shown in Figure 3.6. Moreover, the estimation of the order of convergence indicates the interfacial condition is properly implemented.

In Figure 3.7, the numerical solutions with the dynamic capillary pressure models are compared to the numerical solution obtained with static capillary pressure. The dynamic capillary pressure has substantially different values across the interface with

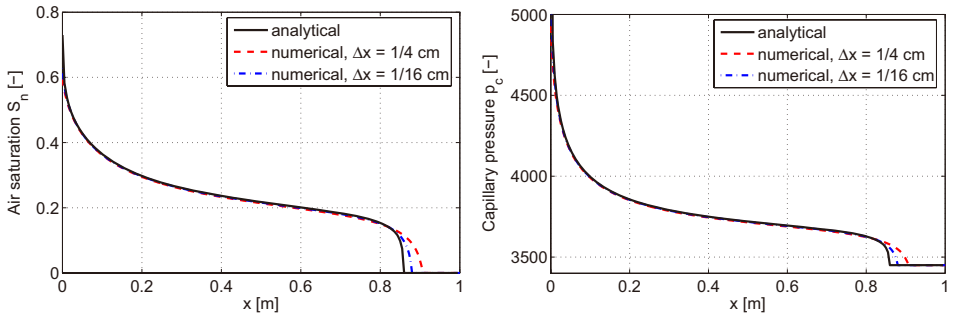

Experimental order of convergence		
Δx $[cm]$	eoc_1	eoc_2
$4 \rightarrow 2$	0 83	0.64
$2 \rightarrow 1$	0.73	0.64
$1 \rightarrow 1/2$	0.75	0.65
$1/2 \rightarrow 1/4$	0.77	0.67
$1/4 \rightarrow 1/8$	0.79	0.68
$1/8 \rightarrow 1/16$	0.81	0.70

Grid size Δx $[cm]$	Time step Δt $[s]$
4	16
2	4
1	1
$1/2$	$1/4$
$1/4$	$1/16$
$1/8$	$1/64$
$1/16$	$1/256$

FIG. 3.4. *Numerical solutions of the advection and capillary diffusion problem in homogeneous porous medium, $t = 1000$ s. The experimental order of convergence eoc_1 and eoc_2 are measured in L_1 and L_2 norms, respectively.*

respect to the static capillary pressure, which is in contradiction to [18].

Initial condition :	$S_n(x,0) = 0.73$	$\forall x \in (0, L/2)$
	$S_n(x,0) = 0$	$\forall x \in (L/2, L)$
Boundary conditions :	$S_n(0,t) = 0.73$	$\forall t \in [0,T]$
	$S_n(L,t) = 0$	$\forall t \in [0,T]$
Problem setup :	$T = 1000$ s, $L = 2$ m, $g = 0$	
Capillary pressure :	Classical model (1.3), $p_c \equiv p_c^{eq}$, $\tau \equiv 0$	
Porous medium :	Heterogeneous porous medium	
Sands :	Ohji sand, Table 3.1	in $(0, L/2)$
	$\text{Ohji}_{0.9}$ sand Table 3.1	in $(L/2, 0)$

TABLE 3.7
Description of the pure capillary diffusion problem in heterogeneous porous medium.

3.5. Advection and capillary diffusion in heterogeneous medium. In 2008, Fučík et al. [11] generalized the van Duijn and de Neef problem formulation by the inclusion of the McWhorter and Sunada solution in homogeneous porous medium. The resulting problem formulation requires that the van Duijn and de Neef initial saturation distribution and the McWhorter and Sunada boundary fluxes are prescribed, see Table 3.8.

In Figure 3.8, the numerical solutions are compared to the semi-analytical solution and the experimental error of convergence is shown.

The numerical solutions of the problem for the dynamic capillary pressure models are shown in Figure 3.9.

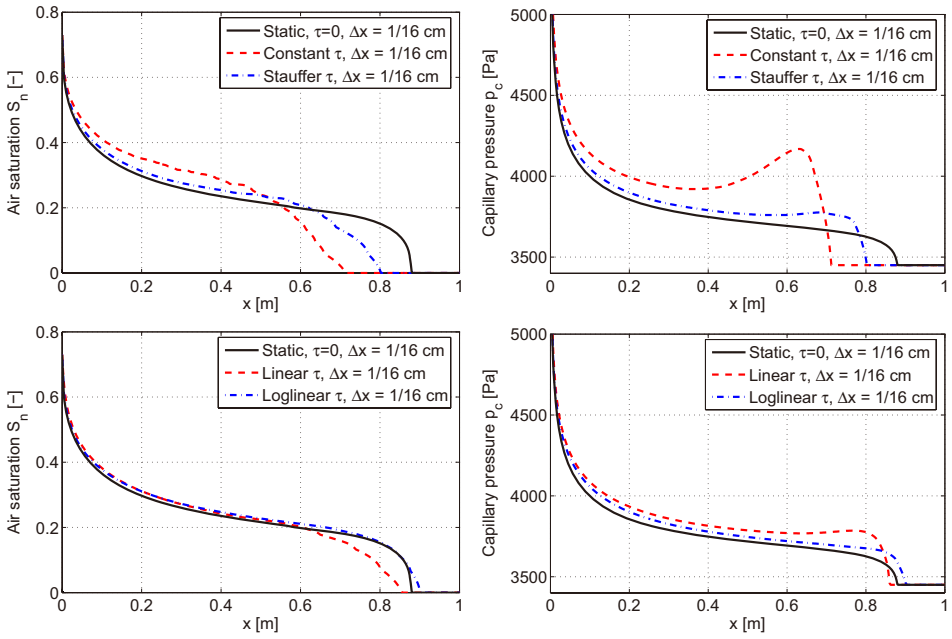

FIG. 3.5. *Numerical solutions of the advection and capillary diffusion problem in homogeneous porous medium using the constant, linear, and loglinear models for dynamic effect coefficient τ are compared to the numerical solutions obtained for the static capillary pressure $\tau = 0$, $t = 1000$ s.*

Problem description		
Initial condition :	$S_n(x,0) = 0.73$	$\forall x \in (0, L/2)$
	$S_n(x,0) = 0$	$\forall x \in (L/2, L)$
Boundary conditions :	$S_n(0,t) = 0.73$	$\forall t \in [0,T]$
	$S_n(L,t) = 0$	$\forall t \in [0,T]$
	$p_n(0,t) = \text{const} = 0$	$\forall t \in [0,T]$
	$u_w(L,t) + u_n(L,t) = 1.59 \cdot 10^{-3} t^{-1/2}$	$\forall t \in [0,T]$
Problem setup :	$T = 1000$ s, $L = 2$ m, $g = 0$	
Capillary pressure :	Classical model (1.3), $p_c \equiv p_c^{eq}$, $\tau \equiv 0$	
Porous medium :	Heterogeneous porous medium	
Sands :	Ohji sand, Table 3.1	in $(0, L/2)$
	$\text{Ohji}_{0.9}$ Table 3.1	in $(L/2, 0)$

TABLE 3.8
Description of the advection and capillary diffusion problem in heterogeneous porous medium.

3.6. Discussion of the results. The numerical scheme (2.2) was tested against five different analytical or semi-analytical solutions in the previous subsections. In all cases, the numerical solutions converge towards the analytical or semi-analytical solution and the order of convergence is shown in Figures 3.1, 3.2, 3.4, 3.6, and 3.8.

As expected, the numerical approximation of the discontinuous fronts are not sharp even if the advection term dominates the flow (Figures 3.1, 3.4, and 3.8). This is caused by the numerical diffusion in the scheme (2.2) as it is already described in literature, see [19].

As shown in Figures 3.6 and 3.8, the jump in saturations across the interface in the

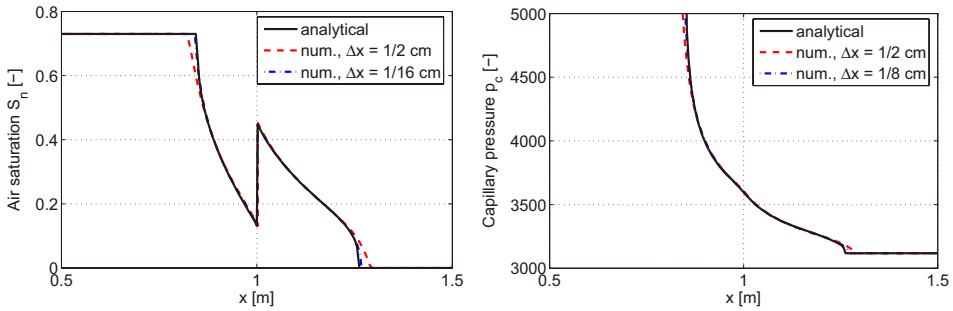

Experimental order of convergence		
Δx $[cm]$	eoc_1	eoc_2
$1 \rightarrow 1/2$	0.83	0.60
$1/2 \rightarrow 1/4$	0.89	0.66
$1/4 \rightarrow 1/8$	0.93	0.70
$1/8 \rightarrow 1/16$	0.93	0.68
$1/16 \rightarrow 1/32$	0.91	0.53

Grid size Δx $[cm]$	Time step Δt $[s]$
1	256
$1/2$	16
$1/4$	4
$1/8$	1
$1/16$	$1/4$
$1/32$	$1/16$

FIG. 3.6. *Numerical solutions of the van Duijn and de Neef problem (the capillary diffusion case in a heterogeneous porous medium), $t = 1000$ s. The experimental order of convergence eoc_1 and eoc_2 are measured in L_1 and L_2 norms, respectively.*

case of the heterogeneous porous medium is determined correctly and, moreover, the presence of a heterogeneity does not influence the experimental order of convergence. This will be an important referential solution for further investigation of the interfacial condition (1.6) in highly heterogeneous porous media.

The inclusion of the dynamic capillary pressure models (constant, linear, and loglinear models of τ) is important in cases, where there is a significant temporal change in the saturation S_n since the temporal derivative of S_n is multiplied by the dynamic effect coefficient τ, see (1.4). This occurs when the advection together with the capillary diffusion dominate the displacement as it is shown in Figures 3.3 and 3.5.

As shown in Figure 3.5, the use of the constant model for the dynamic effect coefficient τ changes the monotonicity of the capillary pressure profile which may be physically unrealistic. Therefore, the constant model requires further investigation of its validity. On the other hand, the use of the linear and the loglinear models of τ does not seem to be important in the homogeneous porous medium since the air saturation and capillary pressure profiles are similar to the profiles computed with the static capillary pressure (compare Figures 3.3 and 3.5).

In the case of a heterogeneous medium, the inclusion of the dynamic capillary pressure may substantionally change the simulated evolution of the flow since the entry pressure of the finer porous media can be achieved sooner or later than in the static case as it is shown in Figures 3.7 and 3.9. This indicates that the conclusions published for the case of Richards equation in [18] may not hold for the full system of equation of the two-phase flow.

4. Conclusion. This manuscript presents a one-dimensional numerical scheme of two-phase incompressible and immiscible flow that enables for simulating non static capillary pressure models in both homogeneous and heterogeneous porous media. The numerical scheme is validated and its order of convergence is estimated using the

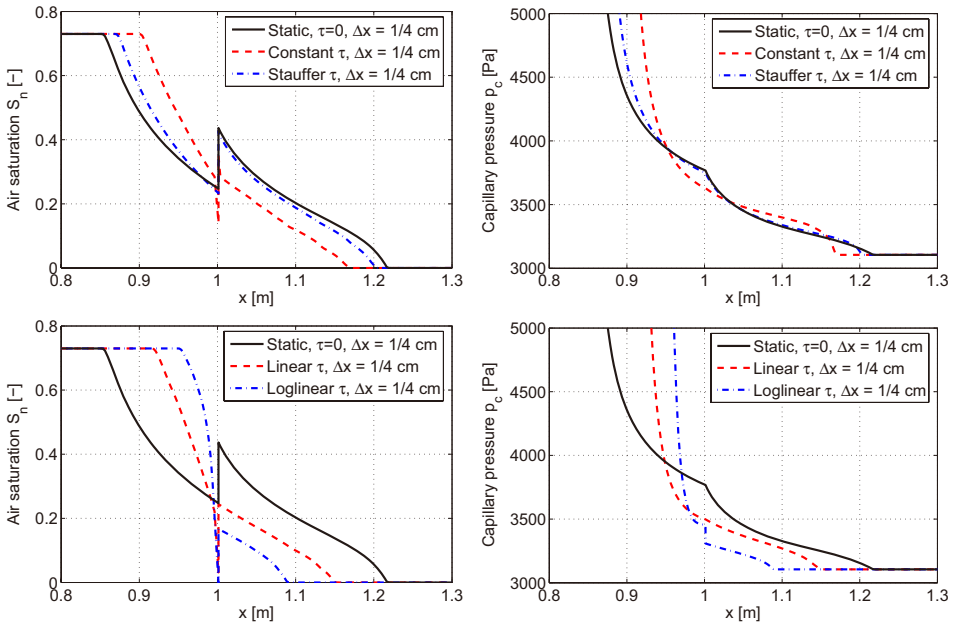

FIG. 3.7. *Numerical solutions of the capillary diffusion problem using the constant, linear, and loglinear models for dynamic effect coefficient τ are compared to the numerical solutions obtained for the static capillary pressure $\tau = 0$ in a heterogeneous porous medium, $t = 1000$ s.*

analytical and semi-analytical solutions for advection, advection and diffusion, and diffusion dominated problems, respectively.

Laboratory measured parameters were used in the numerical simulation of the dynamic capillary pressure including three main models of the dynamic effect coefficient $\tau = \tau(S_w)$ - constant, linear, and loglinear. The numerical solutions for the dynamic capillary pressure show that the dynamic effect has significant impact on the magnitude of the capillary pressure while the change in the saturation profiles may be considered negligible in some cases. The constant model of τ showed rather unrealistic profile of the numerical approximation of the capillary pressure because the spatial monotonicity was different with respect to the results obtained with the static capillary pressure model.

Results of the simulation indicate that the dynamic effect may not be so important in drainage problems in a homogeneous porous medium, but, on the other hand, it is of a great importance in highly heterogeneous media where the capillarity governs flow through material interfaces.

5. List of symbols.

Acknowledgement. This work has been supported by:

- Project "Applied Mathematics in Technical and Physical Sciences" MSM 6840770010, Ministry of Education of the Czech Republic.
- Project "Mathematical Modelling of Multiphase Porous Media Flow" 201/08/P567 of the Czech Science Foundation (GA ČR).

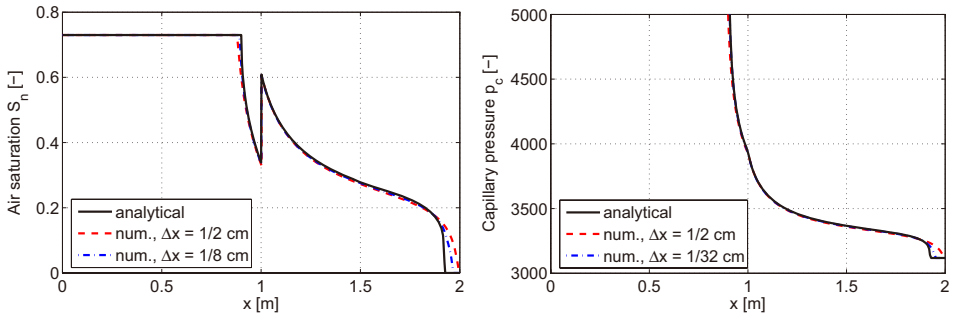

Experimental order of convergence		
Δx $[cm]$	eoc_1	eoc_2
$2 \rightarrow 1$	0.88	0.61
$1 \rightarrow 1/2$	0.89	0.64
$1/2 \rightarrow 1/4$	0.90	0.67
$1/4 \rightarrow 1/8$	0.92	0.69
$1/8 \rightarrow 1/16$	0.92	0.69
$1/16 \rightarrow 1/32$	0.91	0.63

Grid size Δx $[cm]$	Time step Δt $[s]$
2	16
1	4
$1/2$	1
$1/4$	$1/4$
$1/8$	$1/16$
$1/16$	$1/64$
$1/32$	$1/256$

FIG. 3.8. *Numerical solutions of the advection and capillary diffusion problem in heterogeneous porous medium, $t = 1000$ s. The experimental order of convergence eoc_1 and eoc_2 are measured in L_1 and L_2 norms, respectively.*

Symbol	Units	Description
S_α	$[-]$	Saturation
p_α	$[ML^{-1}T^{-2}]$	Pressure
ρ_α	$[ML^{-3}]$	Density
μ_α	$[ML^{-1}T^{-1}]$	Dynamic viscosity
g	$[LT^{-2}]$	Gravitational acceleration
Φ	$[-]$	Porosity
K	$[L^2]$	Intrinsic conductivity
$k_{r\alpha}$	$[-]$	Relative permeability
τ	$[ML^{-1}T^{-1}]$	Dynamic effect coefficient
α	w, n	Index of wetting or non-wetting fluid

TABLE 5.1
List of symbols

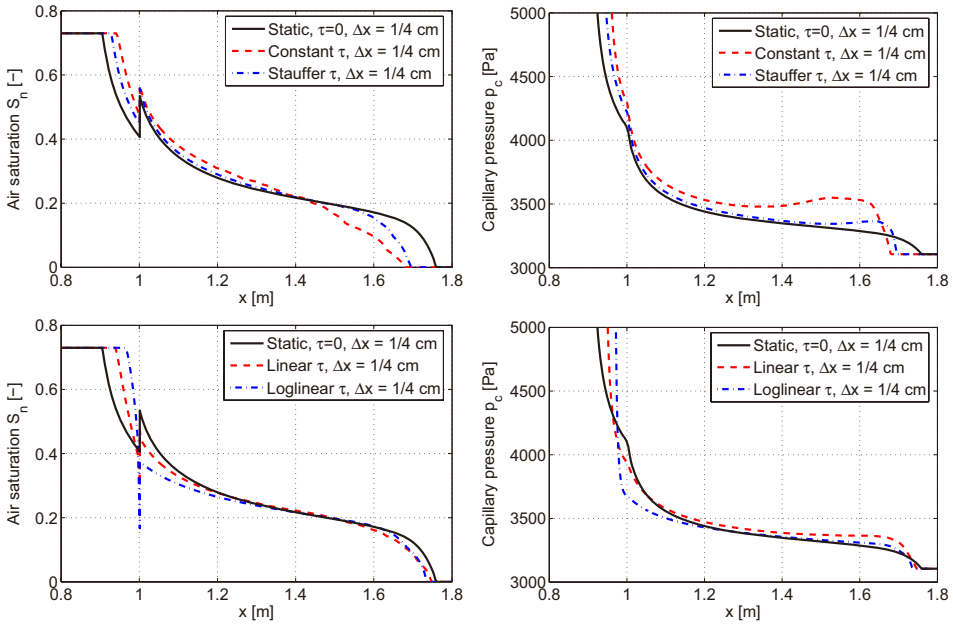

FIG. 3.9. *Numerical solutions of the advection and capillary diffusion problem in heterogeneous porous medium using the constant, linear, and loglinear models for dynamic effect coefficient τ are compared to the numerical solutions obtained for the static capillary pressure $\tau = 0$, $t = 1000$ s.*

REFERENCES

[1] P. Bastian. *Numerical Computation of Multiphase Flows in Porous Media*. Habilitation Dissertation, Kiel university (1999).

[2] J. Bear and A. Verruijt. *Modeling Groundwater Flow and Pollution*. D. Reidel, Holland, Dordrecht, (1990).

[3] A. Beliaev and S. Hassanizadeh. *A Theoretical Model of Hysteresis and Dynamic Effects in the Capillary Relation for Two-phase Flow in Porous Media*. Transport in Porous Media **43** (2001), 487–510.

[4] R. H. Brooks and A. T. Corey. *Hydraulic properties of porous media*. Hydrology Paper **3** (1964), 27.

[5] S. Buckley and M. Leverett. *Mechanism of fluid displacement in sands*. Trans. AIME **146** (1942), 107–116.

[6] H. Dahle, M. Celia, and S. Majid Hassanizadeh. *Bundle-of-Tubes Model for Calculating Dynamic Effects in the Capillary-Pressure-Saturation Relationship*. Transport in Porous Media **58** (2005), 5–22.

[7] D. Das, S. Hassanizadeh, B. Rotter, and B. Ataie-Ashtiani. *A Numerical Study of Micro-Heterogeneity Effects on Upscaled Properties of Two-Phase Flow in Porous Media*. Transport in Porous Media **56** (2004), 329–350.

[8] R. Fučík. *Numerical Analysis of Multiphase Porous Media Flow in Groundwater Contamination Problems , Graduate Thesis*. FNSPE of Czech Technical University Prague, Prague, (2006).

[9] R. Fučík, M. Beneš, J. Mikyška, and T. H. Illangasekare. Generalization of the benchmark solution for the two-phase porous-media flow. In 'Finite Elements Models, MODFLOW, and More : Solving Groundwater problems', 181–184, (2004).

[10] R. Fučík, J. Mikyška, M. Beneš, and T. Illangasekare. *An Improved Semi-Analytical Solution for Verification of Numerical Models of Two-Phase Flow in Porous Media*. Vadose Zone Journal **6** (2007), 93–104.

[11] R. Fučík, J. Mikyška, M. Beneš, and T. Illangasekare. *Semianalytical Solution for Two-Phase Flow in Porous Media with a Discontinuity*. Vadose Zone Journal **7** (2008), 1001.

[12] R. Fučík, J. Mikyška, and T. H. Illangasekare. *Evaluation of saturation-dependent flux on two-phase flow using generalized semi-analytic solution*. Proceedings on the Czech Japanese Seminar in Applied Mathematics (2004), 25–37.

[13] W. Gray and S. Hassanizadeh. *Paradoxes and Realities in Unsaturated Flow Theory*. Water Resources Research **27** (1991), 1847–1854.

[14] W. Gray and S. Hassanizadeh. *Unsaturated Flow Theory Including Interfacial Phenomena*. Water Resources Research **27** (1991), 1855–1863.

[15] S. Hassanizadeh, M. Celia, and H. Dahle. *Dynamic Effect in the Capillary Pressure-Saturation Relationship and its Impacts on Unsaturated Flow*. Vadose Zone Journal **1** (2002), 38–57.

[16] S. Hassanizadeh and W. Gray. *Thermodynamic basis of capillary pressure in porous media*. Water Resources Research **29** (1993), 3389–3406.

[17] R. Helmig. *Multiphase Flow and Transport Processes in the Subsurface : A Contribution to the Modeling of Hydrosystems*. Springer Verlag, Berlin, (1997).

[18] O. Ippisch, H. Vogel, and P. Bastian. *Validity limits for the van Genuchten-Mualem model and implications for parameter estimation and numerical simulation*. Advances in Water Resources **29** (2006), 1780–1789.

[19] R. LeVeque and I. NetLibrary. *Finite Volume Methods for Hyperbolic Problems*. Cambridge University Press, (2002).

[20] S. Manthey. *Two-phase flow processes with dynamic effects in porous media - parameter estimation and simulation*. Institut fur Wasserbau der Universitat Stuttgart, Stutgart, (2006).

[21] S. Manthey, S. Majid Hassanizadeh, and R. Helmig. *Macro-Scale Dynamic Effects in Homogeneous and Heterogeneous Porous Media*. Transport in Porous Media **58** (2005), 121–145.

[22] D. McWhorter and D. Sunada. *Exact Integral Solutions for Two-Phase Flow*. Water Resources Research **26** (1990), 399–413.

[23] J. Mikyška. *Numerical Model for Simulation of Behaviour of Non-Aqueous Phase Liquids in Heterogeneous Porous Media Containing Sharp Texture Transitions, Ph.D. Thesis*. FNSPE of Czech Technical University, Prague, (2005).

[24] M. Peszyńska and S. Yi. International Journal of Numerical Analysis and Modeling **5** (2008), 126–149.

[25] T. Sakaki, D. O'Carroll, and T. Illangasekare. *Direct laboratory quantification of dynamic coefficient of a field soil for drainage and wetting cycles*. American Geophysical Union,

Fall Meeting 2007, abstract# H53F-1486 (2007).
[26] F. Stauffer. Time dependence of the relations between capillary pressure, water content and conductivity during drainage of porous media. In 'On scale effects in porous media, IAHR, Thessaloniki, Greece', (1978).
[27] C. van Duijn and M. de Neef. *Self-similar Profiles for Capillary Diffusion Driven Flow in Heterogeneous Porous Media*. Centrum voor Wiskunde en Informatica, (1996).
[28] M. T. van Genuchten. *A closed-form equation for predicting the hydraulic conductivity of unsaturated soils.* Soil Science Society of America Journal **44** (1980), 892–898.